J Sol-Gel Sci Technol (2015) 76:74–81
DOI 10.1007/s10971-015-3753-x

ORIGINAL PAPER

Microwave rapid conversion of sol–gel-derived hydroxyapatite into β-tricalcium phosphate

Mohamad Nageeb Hassan[1,2] · Morsi Mohamed Mahmoud[3,4] · Ahmed Abd El-Fattah[1] · Sherif Kandil[1]

Received: 14 February 2015 / Accepted: 19 May 2015 / Published online: 28 May 2015

Abstract Calcium phosphate-based biomaterials are of great interest due to their use in various biomedical applications. Current preparation methods of β-tricalcium phosphate (β-TCP) require the processing of calcium phosphate precursors at high temperatures for long periods. Sol–gel-derived calcium-deficient carbonated hydroxyapatite (CHA) samples were synthesized and then aged at different times (24 and 90 h), while other freshly prepared samples were subjected to microwave (MW) radiation for 10 min in order to prepare β-TCP. All samples were calcined (at 750 °C) and then were characterized using scanning electron microscopy, Fourier transform infrared spectroscopy and X-ray diffraction. The 24-h-aged samples showed complete degradation into β-TCP and calcium pyrophosphate (CPP) phases. However, only β-TCP phase was detected in the 90-h-aged samples. Furthermore, β-TCP as the major phase was also obtained in the 10-min MW-treated unaged samples. The aging of sol–gel-derived CHA samples for 90 h had a positive effect on the conversion of CHA into β-TCP phase. Furthermore, the MW treatment of the unaged CHA samples enhanced its total conversion into β-TCP in shorter time which could be attributed to the MW irradiation-induced effect on the CHA structure.

Graphical Abstract

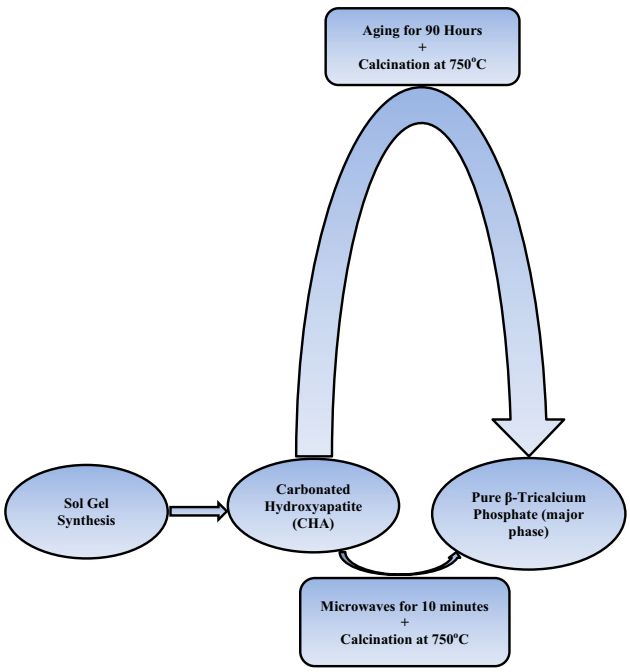

Keywords Sol–gel · Microwave processing · Aging · Hydroxyapatite · β-Tricalcium phosphate

✉ Morsi Mohamed Mahmoud
morsi.ahmed@kit.edu

[1] Department of Materials Science, Institute of Graduate Studies and Research, Alexandria University, El-Shatby, Alexandria 21526, Egypt

[2] Department of Dental Biomaterials, Faculty of Dentistry, Alexandria University, El-Azarita, Alexandria 21526, Egypt

[3] Institute for Applied Materials - Applied Materials Physics (IAM-AWP), Karlsruhe Institute of Technology (KIT), Hermann-von-Helmholtz-Platz 1, 76344 Eggenstein-Leopoldshafen, Germany

[4] Advanced Technology and New Materials Research Institute (ATNMRI), City of Scientific Research and Technological Application (SRTA), New Borg Al-Arab City, Alexandria 21934, Egypt

1 Introduction

Calcium phosphate-based biomaterials have been used frequently as bone substitutes and osteoconductive scaffolds due to their chemical similarity to the inorganic phase of bone [1]. Currently, they are widely used to promote bone repair and regeneration instead of autogenous (self) bone graft/flab transplantation used for orthopedics, oral and maxillofacial bone defects [2] or implant coatings [3]. Calcium phosphates (CAP) exist in different forms and phases including hydroxyapatite (HA), calcium-deficient HA, tricalcium phosphates (α or β-TCP), calcium monophosphate and biphasic calcium phosphate (BCP) [4]. Carbonated hydroxyapatite (CHA) differs from stoichiometric HA in which carbonate ions substitute for the hydroxyl ion (A type) or phosphate ion (B type) in the apatite structure [5]. Although CHA is more similar to the biological apatites [6], it shows a reduced crystallinity percent, sintering and decomposition temperatures when compared to stoichiometric HA [5, 7].

CHA prepared via sol–gel method offers a distinct advantage of a molecular-level mixing of the calcium and phosphorus precursors, which improves the yield and the chemical homogeneity of the resulting CHA [8]. Furthermore, the high reactivity of the sol–gel powders usually results in the decrease in the heat treatment and the sintering temperatures [9].

β-Tricalcium phosphate (β-TCP) has been used recently as bone and tooth implants due to its unique biocompatibility, osteoconductivity and bioresorbability [10, 11]. β-TCP is mainly prepared via solid-state [12, 13] and wet-chemical methods [14]. In order to synthesize β-TCP, the current preparation methods require the heating of calcium phosphate precursors for very long periods [15] (>24 h) and/or at very high temperatures (up to 1000 °C) [13, 16–18].

Microwave (MW) processing of materials is an advanced processing technology with several advantages [19, 20]. It provides a powerful and significantly different tool to process materials and in most cases improves the performance characteristics of the existing materials. These anticipated benefits include more precise and controlled volumetric heating, faster ramp-up to temperature, lower energy consumption, and enhanced quality and properties of the processed materials [21, 22]. Nano-structured calcium phosphates can be better tailored to obtain desired chemical compositions, surface properties (specifically topography), mechanical properties and distribution of grain size similar to those of physiological bone (which contains 70 % by weight of HA ceramic with grain sizes <100 nm) [23]. MW-assisted synthesized nano-HA was approved for its cell biocompatibility [24] and the ability of bioresorption in stimulated body fluid with a dissolution rate fairly higher than conventional HA and closer to biological apatite due to its nano-structure processing [25]. Others investigated the effects of micro-sized MW synthesized versus nano-sized conventionally precipitated HA (μ/n-HA) on the osteogenic differentiation of rat bone marrow-derived mesenchymal stem cells (rBMSCs) [26]. It was shown that rBMSCs expressed higher levels of osteoblast-related markers with nHA than μ-HA stimulation; thus, the size of calcium phosphates used is an important factor for affecting the osteogenic differentiation of rBMSCs and to obtain more committed differentiated cells. The purpose of the current study was to investigate the possibility to prepare β-TCP from sol–gel-derived CHA via two different routes, the MW treatment and the aging techniques.

2 Materials and methods

2.1 Sol–gel synthesis, aging and MW treatment

For the synthesis of the CHA, calcium nitrate tetrahydrate ($Ca(NO_3)_2{\cdot}4H_2O$) and ammonium dihydrogen phosphate ($(NH_4)H_2PO_4$) were used as the starting materials for Ca and P (Oxford Chemicals, India). Sol–gel-derived CHA samples were reported recently by Bakan et al. [27] and were prepared according to the protocol. In the synthesis process, a solution of $Ca(NO_3)_2{\cdot}4H_2O$ in ethanol (1.67 M) was prepared, whereas ammonium hydroxide $(NH_4)OH$ was used to adjust the pH of the solution (pH = 10) (solution A). On the other hand, a solution of $(NH_4)H_2PO_4$ (1 M) was prepared and adjusted at pH = 10 (solution B). Solution A was added drop wise to solution B (in equal volumes) at a constant rate (1 mL/min) under vigorous stirring at room temperature, in which the total Ca/P feed ratio = 1.67. Immediately after the solution has transformed into gel, the rate of stirring was adjusted to keep vigorous stirring. A flow chart shown in Fig. 1 outlines the experimental procedure and conditions used to prepare four groups of samples.

The as-prepared group was just dried, neither aged nor calcined. Groups A and B were subjected to an aging process for 24 and 90 h, respectively. Group C was subjected to MW treatment for 10 min using a domestic MW oven working at 2.45 GHz and using 80 % power of the total 1400 W. The three groups (A, B and C) were dried at 80 °C for 12 h and then calcined at 750 °C for 4 h using an electrical furnace at a heating rate of 10 °C/min in air.

2.2 Characterization of the processed CHA samples

All groups were characterized using scanning electron microscopy (SEM). The morphology of the prepared samples (gold coated) was observed using SEM (JEOL 5300-JSM-Japan) operated at 30 keV. Semi-quantitative analyses of the chemical composition of CHA and β-TCP samples were

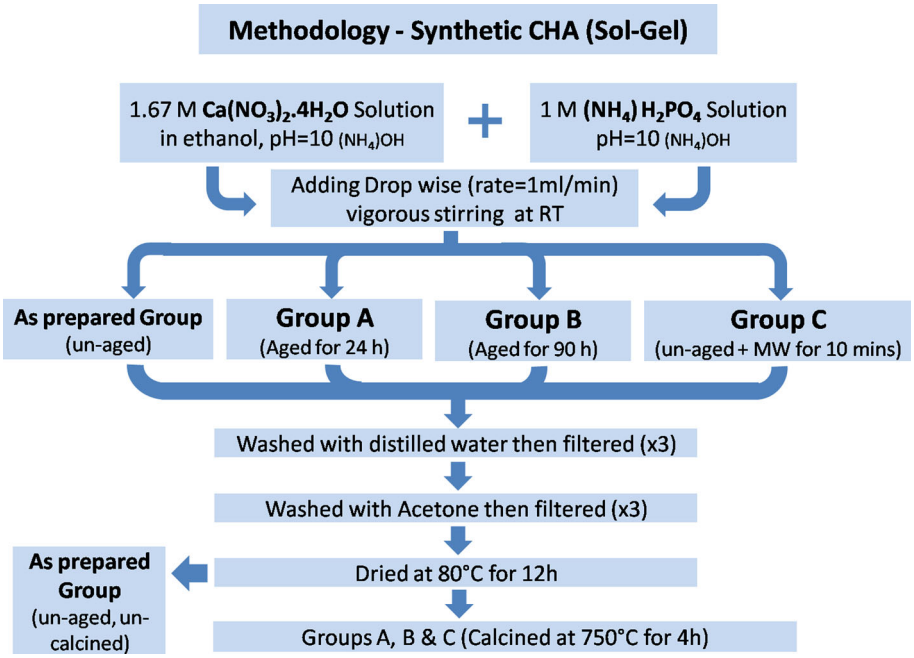

Fig. 1 Schematic of the methodology to prepare synthetic CHA via sol–gel, classified into four groups

conducted by EDX (energy-dispersive X-ray spectroscopy). Analysis was performed on uncoated powder samples at 15 kV for 60 s. Ca/P mole ratios of the samples were determined as the average of five random runs on each sample. The samples were analyzed using a spectrum 100 FT-IR spectrometer (Perkin Elmer–USA) using KBr pellet technique, wave number region 400–4000 cm^{-1}. XRD was performed using an X'pert diffractometer (Philips–Netherlands), 2θ ranging from 2° to 60°. The phases were identified and compared with the literature reports as well as the Joint Committee on Powder Diffraction Standards (JCPDS) for calcium phosphate samples: CHA, β-TCP and CPP with the PDF numbers: 74-0566, 70-2065 and 45-1016, respectively.

3 Results

In sol–gel synthesis of CHA, the pH of the reactant solutions was found to be very critical. When the pH was lower than 10, a very poor precipitation of amorphous white precipitant with very low yield was observed. On the other hand, solutions adjusted at pH = 10 produced an immediate gel (when added drop wise).

3.1 Characterization of the CHA samples

3.1.1 Morphological and chemical composition analysis (SEM and EDX)

Scanning electron micrographs of the as-prepared sol–gel-derived powder showed the formation of flakes of highly aggregated spherical calcium-deficient carbonated HA in a submicron size (Fig. 2a). Groups A and B after calcinations (750 °C for 4 h) revealed platelet-like morphology with minor percent of rod-like particles (Fig. 2b, c). For group C, the produced particles appeared to be agglomerated spherical particles (diameter about 200–400 nm) and minor rod-like particles (micro-size) (Fig. 2d). Aging was found to significantly increase the particle size; however, MW-treated samples showed minor increase in particle size. Mixed morphologies were also observed in previous studies [28, 29], where several researchers further used other effective chemical (nucleating agents) [30] and physical agents (ultrasonic waves) [7, 31] to control the size and shape of the produced CHA. The EDX analyses performed on the prepared samples are listed in Table 1. Within the accuracy limits of this method, the as-prepared group was identical to the expected Ca/P ratios of CHA [32], while the MW-treated samples (group C) was very close to the expected Ca/P ratios of pure β-TCP [14] (Fig. 3).

3.1.2 Fourier transform infrared spectroscopy (FT-IR)

The FT-IR spectrum of the as-prepared gel group (unaged, un-calcined) showed the formation of a pure CHA powder when compared with the literature [33] (carbonate and phosphate bands are shown in Fig. 4a). The carbonate ion was formed and detected due to the reaction occurred with the atmospheric carbon dioxide in the alkaline pH solutions (pH = 10). The intensity of $[CO_3]^{-2}$ peaks was decreased at high calcination temperature (>400 °C) due to its release

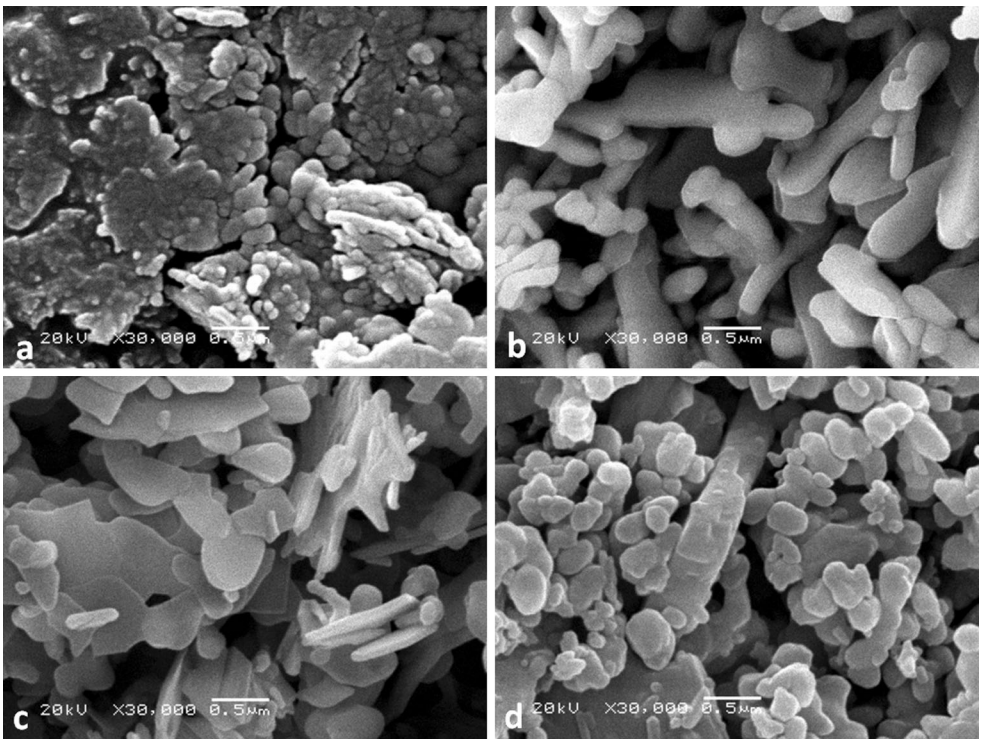

Fig. 2 SEM of the as-prepared synthetic sol–gel-derived CHA (**a**) and the processed groups: **b** group A (aged for 24 h), **c** group B (aged for 90 h) and **d** group C (MW treated)

Table 1 Mean atomic Ca/P ratio values of the prepared samples using EDX

Sample	Ca/P ratio
As-prepared group	1.58
Group A	1.49
Group B	1.59
Group C	1.51

as volatile gases [34]. The residual nitrate group (NO_3^-) was not detected (peaks 820 and 1380 cm^{-1}) as it was removed through washing [27].

The FT-IR spectrum of group A (aged for 24 h and calcined at 750 °C) revealed that the $[PO_4]^{-3}$ band around 1000 cm^{-1} has appeared with peaks at 1034, 1070 and 1097 cm^{-1} which was attributed to the asymmetric stretching of (O–P–O). A medium intensity band at about 970 cm^{-1} which correspond to the symmetric stretching (O–P–O) indicated the degradation of CHA (Fig. 4b) [35]. In addition to the complete dehydration (absence of OH^- peak at 1640 cm^{-1}) and the removal of carbonate ions from the apatite structure, the appearance of peaks at 947 and 975 cm^{-1} (Fig. 4b, arrows) was characteristic of the presence of β-TCP [36]. The peak at 1215 cm^{-1} was due to the bending mode of the hydrogen belonging to the group ($–O_3PO–H–O–PO_3$) [35], while the peaks at 748 and 1165 cm^{-1} indicated the formation of calcium pyrophosphate (CPP) with P_2O_7 group [37]. These results are also in accordance with previous reports indicating that the prepared CHA decomposes into β-TCP and CPP and calcium hydrogen phosphate when calcined at temperature above 600 °C [34].

A similar decomposition of CHA was detected for group B samples (aged for 90 h) (Fig. 4c); however, the bands of CPP (748 and 1165 cm^{-1}) were nearly absent. This indicates the formation of β-TCP phase which could be attributed to the positive effect of aging on the properties of sol–gel-derived CHA [27]. On the other hand, group C (Fig. 4d) showed almost the same peaks as in group B with wider (PO_4) peak around 1000 cm^{-1} which is characteristic to the formed β-TCP.

3.1.3 X-ray diffraction (XRD)

The XRD phase analysis pattern of all groups compared with the original β-TCP pattern are shown in Fig. 5. The as-prepared group (Fig. 5b) was identical to the HA/CHA with all its major peaks and in the absence of any other phases (JCPDS-PDF no. 74-0566) [34]. The broad patterns at (002) and (211) indicate that the crystallites are very tiny in nature [33]. The produced CHA was not thermally stable, as it degrades into major amounts of β-TCP and minor amounts of CPP and CaO when calcined at 750 °C (group A) (Fig. 5c) [34]. However, the XRD pattern for

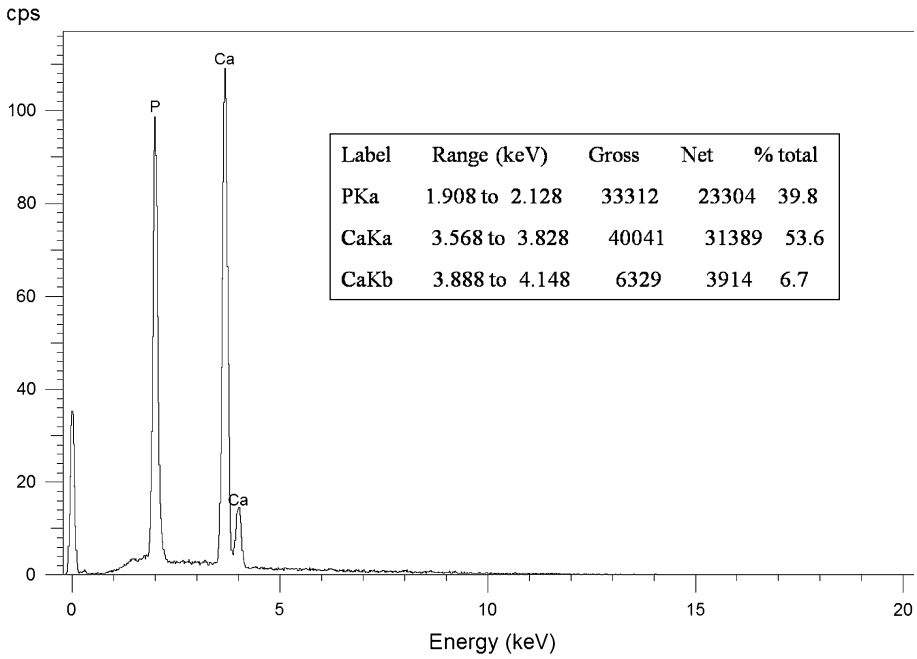

Fig. 3 EDX of the MW-treated sol–gel-derived β-TCP powder (group C)

group B powder (90-h aging) (Fig. 5d) showed much higher content of the formed β-TCP that appeared as the dominant phase (JCPDS-PDF no. 70-2065). This indicates that the phase type and structure of the sol–gel-derived CHA are dependent on the aging time that affects its phase maturation [9]. On the other hand, group C (unaged, MW-treated for just 10 min) showed the development of pure β-TCP after calcination without the need of any aging time (Fig. 5e). Results also confirmed the absence of any other minor phases (e.g., octacalcium phosphate that appear around 5° (2θ) form the final β-TCP product.

4 Discussion

Previous studies have demonstrated that pure carbonated HA could be rapidly synthesized after exposing a freshly prepared solution of biphasic HA/β-TCP (under reflux) to sufficient MW radiation power [38]. This was attributed to the assisting of the deaquation necessary to the formation of apatite in aqueous solution via the MW energy that diminishes the bond between the Ca and its hydration sphere [7, 38, 39].

On the other hand, the thermal degradation of HA into α/β-TCP, tetra-calcium phosphates (TTCP), CPP and/or CaO has also been widely discussed [40, 41]. The normally precipitated CHA has two types of water: adsorbed water (reversibly lost at low temperature up to 120 °C) and lattice water (irreversibly lost between 400 and 500 °C) [42]. Further dehydroxylation (OH^- loss) should begin when HA is heated at temperatures more than 900 °C leading to further decomposition of HA into oxyapatite (unstable) which upon further heating up to 1200 °C decomposes into β-TCP or TTCP. However, α-TCP and/or CaO are formed only above 1200 °C [40, 43].

Previous studies have also showed that other irradiation-induced phenomena were observed during HA examination by high-resolution electron microscopy [44]. The high-energy electron–crystal interaction was believed to cause a local temperature raise (100–500 °C) of the irradiated particles followed by hydroxyl, Ca and oxygen ions displacement and thus the destruction of HA crystal into CaO [45] or α-TCP [41]. Comparable results were mentioned in a previous study, in which Mg^+-stabilized CHA was treated with domestic MW, in which the produced β-TCP was the dominant phase but not as a pure phase [5]. Similarly, other studies have also reported that β-TCP could be detected as an unstable minor phase when CHA was heated between 600 and 800 °C [46, 47]. This low-temperature phase transition could be related to the fact that CHA was less crystalline than the stoichiometric HA [48].

Furthermore, a single-phase β-TCP powders were previously produced by using a MW-assisted "combustion synthesis (auto ignition)/molten salt synthesis" hybrid route, with Ca/P feed ratio equal 3:2 [18, 49]. Other studies have demonstrated that MW irradiation could reduce the maturation time required for HA phase formation through enhancing the biomimetic process that takes place at long aging time [50].

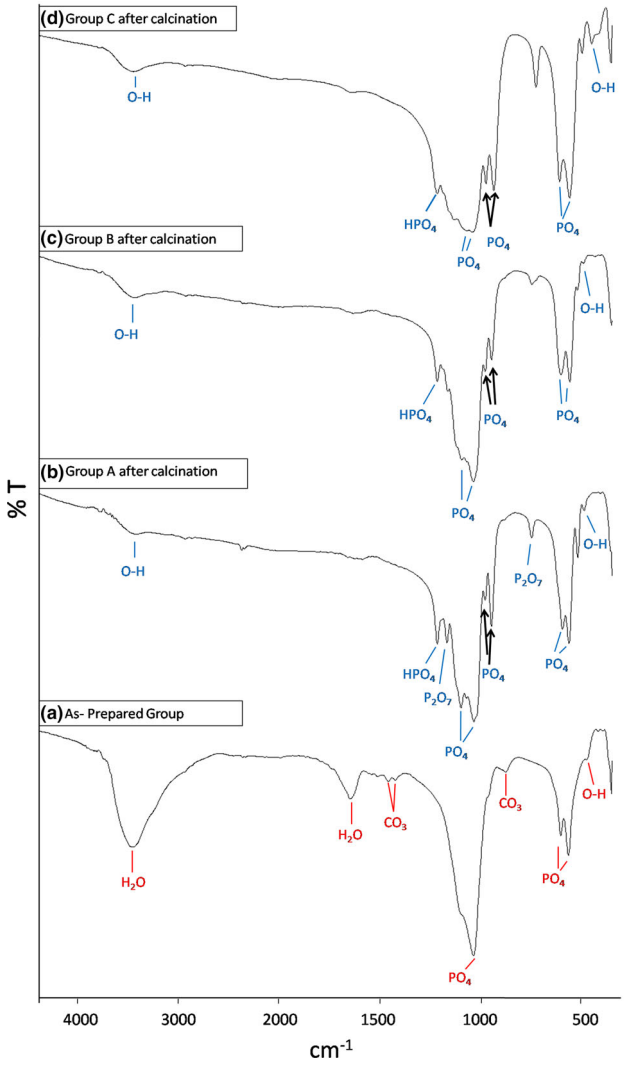

Fig. 4 FT-IR spectrum of the sol–gel-derived CHA samples **a** as-prepared powder (without aging or calcination), **b** group A: powder aged for 24 h. **c** Group B: powder aged for 90 h. **d** Group C: unaged MW-treated powder (10 min). *Arrows* represent the bands of the phosphate groups related to β-TCP phase

In the present study, the MW treatment had reduced the decomposition time of the unaged sol–gel-derived CHA into a stable major β-TCP phase in just 10 min, which had occurred at longer aging times (90 h). This could be attributed to the effect and the interaction of the MW with the CHA particles on the molecular level, especially with water molecules exist on the CHA structure. It is well known and established that the MW energy interacts and heats the water (dipole) molecules very efficiently due to its high dielectric properties [20, 21]. Hence, this interaction resulted in local temperature raise within the CHA structure and reduced the maturation time required for CHA phase, and

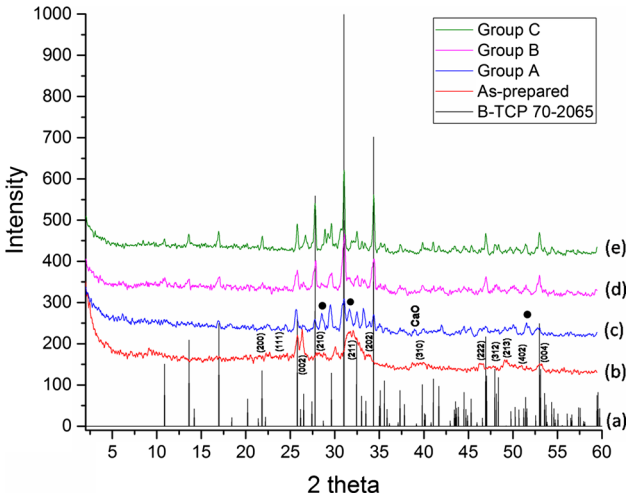

Fig. 5 XRD of the sol–gel-derived powder: *a* β-TCP (JCPDS no. 70-2065) representing the base pattern, *b* CHA (as-prepared group): unaged and un-calcined with indexing. *c* Group A: aged for 24 h and calcined; CPP indicated as (*black circle*). *d* Group B: aged for 90 h and calcined. *e* Group C: unaged MW-treated for 10 min and then calcined

consequently, a rapid transformation and destruction of CHA crystal into β-TCP phase took place [44, 45, 47].

5 Conclusions

Sol–gel method was used to prepare CHA powder. The sol–gel-derived CHA powder was then used to produce β-TCP after calcination via two different methods, aging and MW treatment. Aging of the sol–gel-derived CHA for 24 h caused its degradation into β-TCP with minor amounts of CPP and CaO. Meanwhile, longer aging for 90 h caused the formation of a β-TCP as the major phase with mixed morphologies. This longer aging of the sol–gel-derived CHA samples was having a positive effect on the maturation of the CHA structure so it could be easily converted into β-TCP phase after calcination. On the other hand, the MW treatment (for only 10 min) of the freshly prepared (unaged) CHA showed also the formation of β-TCP as a major phase with highly agglomerated morphology. This rapid conversion could be attributed to the MW irradiation-induced effect on the CHA structure and hence enhance its conversion into β-TCP. The preparation of β-TCP via long-term aging process or via a fast and short MW treatment of the sol–gel-derived CHA was successfully achieved.

Acknowledgments The authors would like to acknowledge the Egyptian Science and Technology Development Fund (STDF) for funding the current study through the Project #6118, STDF-STF agreement. The authors would like to dedicate this work for the soul

of Prof. Moustafa Fakhry Khalil, Professor of Dental Biomaterials, Faculty of Dentistry, Alexandria University.

References

1. Nageeb M, Nouh SR, Bergman K et al (2012) Bone engineering by biomimetic injectable hydrogel. Mol Cryst Liq Cryst 555:177–188. doi:10.1080/15421406.2012.635530
2. Eweida AM, Nabawi AS, Marei MK et al (2011) Mandibular reconstruction using an axially vascularized tissue-engineered construct. Ann Surg Innov Res 5:2. doi:10.1186/1750-1164-5-2
3. Hornberger H, Virtanen S, Boccaccini AR (2012) Biomedical coatings on magnesium alloys—a review. Acta Biomater 8:2442–2455. doi:10.1016/j.actbio.2012.04.012
4. Yang S, Leong KF, Du Z, Chua CK (2001) The design of scaffolds for use in tissue engineering. Part I. Traditional factors. Tissue Eng 7:679–689. doi:10.1089/107632701753337645
5. Kumar TSS, Manjubala I, Gunasekaran J (2000) Synthesis of carbonated calcium phosphate ceramics using microwave irradiation. Biomaterials 21:1623–1629
6. Barakat NAM, Khalil KA, Sheikh FA et al (2008) Physiochemical characterizations of hydroxyapatite extracted from bovine bones by three different methods: extraction of biologically desirable HAp. Mater Sci Eng C 28:1381–1387. doi:10.1016/j.msec.2008.03.003
7. Zou Z, Lin K, Chen L, Chang J (2012) Ultrafast synthesis and characterization of carbonated hydroxyapatite nanopowders via sonochemistry-assisted microwave process. Ultrason Sonochem 19:1174–1179. doi:10.1016/j.ultsonch.2012.04.002
8. Sanosh KP, Chu M, Balakrishnan A, Kim TN (2009) Preparation and characterization of nano-hydroxyapatite powder using sol–gel technique. Bull Mater Sci 32:465–470
9. Liu D-M, Troczynski T, Tseng WJ (2002) Aging effect on the phase evolution of water-based sol–gel hydroxyapatite. Biomaterials 23:1227–1236
10. Wang L, Fan H, Zhang Z-Y et al (2010) Osteogenesis and angiogenesis of tissue-engineered bone constructed by prevascularized β-tricalcium phosphate scaffold and mesenchymal stem cells. Biomaterials 31:9452–9461. doi:10.1016/j.biomaterials.2010.08.036
11. Stiller M, Rack A, Zabler S et al (2009) Quantification of bone tissue regeneration employing beta-tricalcium phosphate by three-dimensional non-invasive synchrotron micro-tomography—a comparative examination with histomorphometry. Bone 44:619–628. doi:10.1016/j.bone.2008.10.049
12. Rangavittal N, Landa-Canovas AR, Gonzalez-Calbet JM, Vallet-Regi M (2000) Structural study and stability of hydroxyapatite and β-tricalcium phosphate: two important bioceramics. J Biomed Mater Res, Part A 51:660–668
13. Ryu H, Youn H, Hong KS et al (2002) An improvement in sintering property of β-tricalcium phosphate by addition of calcium pyrophosphate. Biomaterials 23:909–914
14. Matsumoto N, Yoshida K, Hashimoto K, Toda Y (2010) Preparation of beta-tricalcium phosphate powder substituted with Na/Mg ions by polymerized complex method. J Am Ceram Soc 93:3663–3670. doi:10.1111/j.1551-2916.2010.03959.x
15. Geng F, Tan LL, Jin XX et al (2009) The preparation, cytocompatibility, and in vitro biodegradation study of pure beta-TCP on magnesium. J Mater Sci Mater Med 20:1149–1157. doi:10.1007/s10856-008-3669-x
16. Lin FH, Liao CJ, Chen KS, Sun JS (1998) Preparation of high-temperature stabilized beta-tricalcium phosphate by heating deficient hydroxyapatite with $Na_4P_2O_7 \times 10H_2O$ addition. Biomaterials 19:1101–1107
17. Matsumoto N, Sato K, Yoshida K et al (2009) Preparation and characterization of beta-tricalcium phosphate co-doped with monovalent and divalent antibacterial metal ions. Acta Biomater 5:3157–3164. doi:10.1016/j.actbio.2009.04.010
18. Jalota S, Tas AC, Bhaduri SB (2004) Microwave-assisted synthesis of calcium phosphate nanowhiskers. J Mater Res 19:1876–1881. doi:10.1557/JMR.2004.0230
19. Mahmoud MM, Folz DC, Suchicital CTA, Clark DE (2012) Crystallization of lithium disilicate glass using microwave processing. J Am Ceram Soc 95:579–585. doi:10.1111/j.1551-2916.2011.04936.x
20. Clarke DE, Folz DC, Folgar CE, Mahmoud MM (eds) (2005) Microwave solutions for ceramic engineers, vol 494. The American Ceramic Society, Westerville, Ohio
21. Clark DE, Sutton WH (1996) Microwave processing of materials. Annu Rev Mater Sci 26:299–331. doi:10.1146/annurev.ms.26.080196.001503
22. Agrawal D (2010) Latest global developments in microwave materials processing. Mater Res Innov 14:3–8. doi:10.1179/143307510X12599329342926
23. Webster TJ, Ergun C, Doremus RH et al (2001) Enhanced osteoclast-like cell functions on nanophase ceramics. Biomaterials 22:1327–1333. doi:10.1016/S0142-9612(00)00285-4
24. Kundu PK, Waghode TS, Bahadur D, Datta D (1998) Cell culture approach to biocompatibility evaluation of unconventionally prepared hydroxyapatite. Med Biol Eng Comput 36:654–658
25. Murugan R, Ramakrishna S (2005) Aqueous mediated synthesis of bioresorbable nanocrystalline hydroxyapatite. J Cryst Growth 274:209–213. doi:10.1016/j.jcrysgro.2004.09.069
26. Huang Y, Zhou G, Zheng L et al (2012) Micro-/nano-sized hydroxyapatite directs differentiation of rat bone marrow derived mesenchymal stem cells towards an osteoblast lineage. Nanoscale 4:2484–2490. doi:10.1039/c2nr12072k
27. Bakan F, Laçin O, Sarac H (2013) A novel low temperature sol–gel synthesis process for thermally stable nano crystalline hydroxyapatite. Powder Technol 233:295–302. doi:10.1016/j.powtec.2012.08.030
28. Han J-K, Song H-Y, Saito F, Lee B-T (2006) Synthesis of high purity nano-sized hydroxyapatite powder by microwave-hydrothermal method. Mater Chem Phys 99:235–239. doi:10.1016/j.matchemphys.2005.10.017
29. Lee B-T, Youn M-H, Paul RK et al (2007) In situ synthesis of spherical BCP nanopowders by microwave assisted process. Mater Chem Phys 104:249–253. doi:10.1016/j.matchemphys.2007.02.009
30. Lak A, Mazloumi M, Mohajerani MS et al (2008) Rapid formation of mono-dispersed hydroxyapatite nanorods with narrow-size distribution via microwave irradiation. J Am Ceram Soc 91:3580–3584. doi:10.1111/j.1551-2916.2008.02690.x
31. Poinern G, Brundavanam R, Le XT et al (2011) Thermal and ultrasonic influence in the formation of nanometer scale hydroxyapatite bio-ceramic. Int J Nanomedicine 6:2083–2095
32. Mostafa NY (2005) Characterization, thermal stability and sintering of hydroxyapatite powders prepared by different routes. Mater Chem Phys 94:333–341. doi:10.1016/j.matchemphys.2005.05.011
33. Kuriakose TA, Kalkura SN, Palanichamy M et al (2004) Synthesis of stoichiometric nano crystalline hydroxyapatite by ethanol-based sol–gel technique at low temperature. J Cryst Growth 263:517–523. doi:10.1016/j.jcrysgro.2003.11.057
34. Pattanayak DK, Dash R, Prasad RC et al (2007) Synthesis and sintered properties evaluation of calcium phosphate ceramics. Mater Sci Eng C 27:684–690. doi:10.1016/j.msec.2006.06.021
35. Koutsopoulos S (2002) Synthesis and characterization of hydroxyapatite crystals: a review study on the analytical methods. J Biomed Mater Res 62:600–612. doi:10.1002/jbm.10280

36. Kalita SJ, Verma S (2010) Nanocrystalline hydroxyapatite bioceramic using microwave radiation: synthesis and characterization. Mater Sci Eng C 30:295–303. doi:10.1016/j.msec.2009.11.007
37. Anee TK, Ashok M, Palanichamy M, Kalkura SN (2003) A novel technique to synthesize hydroxyapatite at low temperature. Mater Chem Phys 80:725–730. doi:10.1016/S0254-0584(03)00116-0
38. Nazir R, Iqbal N, Khan AS et al (2012) Rapid synthesis of thermally stable hydroxyapaptite. Ceram Int 38:457
39. Sarig S, Kahana F (2002) Rapid formation of nanocrystalline apatite. J Cryst Growth 237–239:55–59. doi:10.1016/S0022-0248(01)01850-4
40. Tõnsuaadu K, Gross KA, Plūduma L, Veiderma M (2012) A review on the thermal stability of calcium apatites. J Therm Anal Calorim 110:647–659. doi:10.1007/s10973-011-1877-y
41. Ji H, Marquis PM (1991) Modification of hydroxyapatite during transmission electron microscopy. J Mater Sci Lett 10:132–134. doi:10.1007/BF02352825
42. Ivanova TI, Frank-Kamenetskaya OV, Kol'tsov AB, Ugolkov VL (2001) Crystal structure of calcium-deficient carbonated hydroxyapatite. Thermal decomposition. J Solid State Chem 160:340–349. doi:10.1006/jssc.2000.9238
43. Cihlar J, Buchal A, Trunec M (1999) Kinetics of thermal decomposition of hydroxyapatite bioceramics. J Mater Sci 34:6121–6131
44. Nicolopoulos S, Gonzalez-Calbet JM, Alonso MP et al (1995) Characterization by TEM of local crystalline changes during irradiation damage of hydroxyapatite compounds. J Solid State Chem 116:265–274
45. Brrs EF, Hutchison JL, Senger B et al (1991) HREM study of irradiation damage in human dental enamel crystals. Ultramicroscopy 35:305–322
46. Suchanek WL, Shuk P, Byrappa K et al (2002) Mechanochemical–hydrothermal synthesis of carbonated apatite powders at room temperature. Biomaterials 23:699–710. doi:10.1016/S0142-9612(01)00158-2
47. Layrolle P, Ito A, Tateishi T (1998) Sol–gel synthesis of amorphous calcium phosphate and sintering into microporous hydroxyapatite bioceramics. J Am Ceram Soc 81:1421–1428
48. Kee CC, Ismail H, Mohd Noor AF (2013) Effect of synthesis technique and carbonate content on the crystallinity and morphology of carbonated hydroxyapatite. J Mater Sci Technol 29:761–764. doi:10.1016/j.jmst.2013.05.016
49. Wagner DE, Eisenmann KM, Nestor-kalinoski AL, Bhaduri SB (2013) A microwave-assisted solution combustion synthesis to produce europium-doped calcium phosphate nanowhiskers for bioimaging applications. Acta Biomater 9:8422–8432. doi:10.1016/j.actbio.2013.05.033
50. Guha A, Nayar S, Thatoi HN (2010) Microwave irradiation enhances kinetics of the biomimetic process of hydroxyapatite nanocomposites. Bioinspiration Biomim. doi:10.1088/1748-3182/5/2/024001